Formation of a Porous Platinum Nanoparticle Froth for Electrochemical Applications, Produced without Templates, Surfactants, or Stabilizers

Dequan Yang,[†] Shuhui Sun,[‡] Hui Meng,[‡] Jean-Pol Dodelet,[‡] and Edward Sacher*[,†]

Département de Génie Physique, École Polytechnique, Montréal, QC H3C 3A7, Canada, and INRS, Énergie, Matériaux et Télécommunications, Varennes, QC J3X 1S2, Canada

Received March 11, 2008. Revised Manuscript Received May 15, 2008

Pt nanoparticles (NPs), synthesized via the reduction of H_2PtCl_6 by formic acid at 80 °C, formed a nanoporous froth at the upper surface of the aqueous solution in which they were produced. The NPs, brought to the surface by the escape of CO_2 bubbles produced by the reduction, partly coalesced to form a froth film with a porosity >95%. Scanning and transmission electron microscopies were used to characterize the froth morphology and the NP dimensions, and X-ray photoelectron spectroscopy was used to characterize the NP surface chemistry. The froth was found to be composed of 3−5 nm zerovalent Pt NPs. The porous froth films, which could be removed and handled, demonstrated an electroactive surface area of 168 ± 8 m^2/g Pt, more than 4 times that of a commercial colloidal Pt black, and equivalent to that of the best Pt particle/carbon black electrocatalysts.

Introduction

Pt nanostructures, including nanoparticles (NPs), nanowires, and porous thin films, have received considerable attention in recent years because of their importance in applications such as catalysis, biosensors, and fuel cells.[1–5] In the case of fuel cells, nanostructured Pt is an important catalyst for both oxygen reduction and hydrogen or methanol oxidation reactions. A major issue in such applications is to increase the catalytic activity by increasing the surface area of the catalyst deposited on its support. The use of both larger surface area supports, such as porous substrates[6] and porous Pt,[7,8] has been explored.

Several methods have been used to produce nanoporous Pt films. These include the following:

(1) The template method,[7] e.g., the electrodeposition of Pt into a liquid crystal surfactant template. This method permits facile control of the size of the porous structures, although it is difficult and time-consuming to implement and scale up.

(2) Electrochemical dealloying, such as from $Cu_{0.75}Pt_{0.25}$[8a] or ZnPt[8b] alloys. The method is easily manageable,[8c] but the preparation of the binary alloys requires special techniques, such as melting at temperatures of 1000 °C[8a] or electrodeposition from a complex ionic liquid containing $ZnCl_2$.[8b]

(3) Hydrothermally assisted seed growth.[9]

(4) Electrodeposition methods,[10] which are based on electrochemical reduction and the formation of hydrogen bubbles that function as a template to make three-dimensional nanoramified metal depositions. Although an electrodeposition process can easily create a 3D dendritic metal structure, it is very difficult to control the microstructure so as to obtain the desired features.[10b] Recent improvements in processing may overcome some of these disadvantages.

(5) Teng et al.[11] recently reported the synthesis of porous Pt NPs, using Pt acetylacetonate as the precursor, with reduction by 1,2-hexadecanediol at 220 °C.

Here, we describe the straightforward synthesis of a nanoporous froth thin film, made of Pt NPs, at the relatively low temperature of 80 °C, without using templates, stabiliz-

* Corresponding author. E-mail: edward.sacher@polymtl.ca.
[†] Département de Génie Physique, École Polytechnique.
[‡] INRS, Énergie, Matériaux et Télécommunications.

(1) (a) Che, M. *Adv. Catal.* **1989**, *36*, 55. (b) Bond, G.; Thompson, C. D. T. *Catal. Rev.* **1999**, *41*, 319.
(2) Chen, J. Y.; Herricks, T.; Geissler, M.; Xia, Y. N. *J. Am. Chem. Soc.* **2004**, *126*, 10854.
(3) Youm, T. Y.; Niwa, O.; Tiomita, M.; Hirono, S. *Anal. Chem.* **2003**, *75*, 2080.
(4) (a) Pak, S. C.; Penrose, W.; Hesketh, P. J. *Biosens. Bioelectron.* **2001**, *16*, 371. (b) Harris, K. D.; McBride, J. R.; Nietering, K. E.; Brett, M. J. *Sensors Mater.* **2001**, *13*, 225.
(5) (a) Chan, K. Y.; Ding, J.; Ren, J. W.; Cheng, S. A.; Tsang, K. Y. *J. Mater. Chem.* **2004**, *14*, 505. (b) Liu, Z. L.; Ling, X. Y.; Su, X. D.; Lee, J. Y. *J. Phys. Chem. B* **2004**, *108*, 8234. (c) Xiu, Y. K.; Nakagawa, N. *J. Electrochem. Soc.* **2004**, *151*, A1483.
(6) (a) Gloaguen, F.; Leger, J. M.; Lamy, C. *J. Appl. Electrochem.* **1997**, *27*, 1052. (b) Liu, S. H.; Lu, R. F.; Huang, S. J.; Lo, A. Y.; Chien, S. H.; Liu, S. B. *Chem. Commun.* **2006**, *32*, 3435. (c) Rioux, R. M.; Song, H.; Hoefelmeyer, J. D.; Yang, P.; Somorjai, G. A. *J. Phys. Chem. B* **2005**, *109*, 2192.
(7) (a) Jiang, P.; Bertone, J. F.; Colvin, V. L. *Science* **2001**, *291*, 453. (b) Boo, S.; Park, S.; Ku, B. Y.; Park, J. H.; Kim, H. C.; Chung, T. D. *J. Am. Chem. Soc.* **2004**, *126*, 4524. (c) Choi, K. S.; Mcfarland, E. W.; Stucky, G. D. *Adv. Mater.* **2003**, *15*, 2018. (d) Attard, G. S.; Bartlett, P. N.; Coleman, N. R. B.; Elliott, J. M.; Owen, J. R.; Wang, J. H. *Science* **1997**, *278*, 838. (e) Teng, X. W.; Liang, X. Y.; Rahman, S.; Yang, H. *Adv. Mater.* **2005**, *17*, 2237. (f) Fukuoka, A.; Araki, H.; Sakamoto, Y.; Sugimoto, N.; Tsukada, H.; Kumai, Y.; Akimoto, Y.; Ichikawa, M. *Nano Lett.* **2002**, *2*, 793.
(8) (a) Pugh, D. V.; Dursun, A.; Corcoran, S. G. *J. Mater. Res.* **2003**, *18*, 216. (b) Huang, J. F.; Sun, I. W. *Chem. Mater.* **2004**, *16*, 1829. (c) Liu, H. T.; He, P.; Li, Z. Y.; Li, J. H. *Nanotechnology* **2006**, *17*, 2167.
(9) Peng, X. S.; Koczkur, K.; Nigro, S.; Chen, A. C. *Chem Commun.* **2004**, *24*, 2872.
(10) (a) Zach, M. P.; Penner, M. *Adv. Mater.* **2000**, *12*, 878. (b) Shin, H. C.; Dong, J.; Liu, M. L. *Adv. Mater.* **2003**, *15*, 1610.
(11) Teng, X.; Liang, X. Y.; Maksimuk, S.; Yang, H. *Small* **2006**, *2*, 249.

10.1021/cm800713g CCC: $40.75
Published on Web 06/20/2008

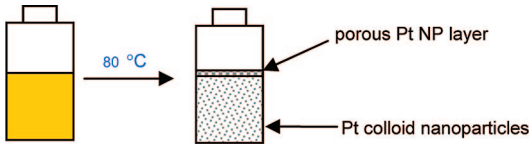

Figure 1. Porous Pt NP froth preparation during H_2PtCl_6 reduction.

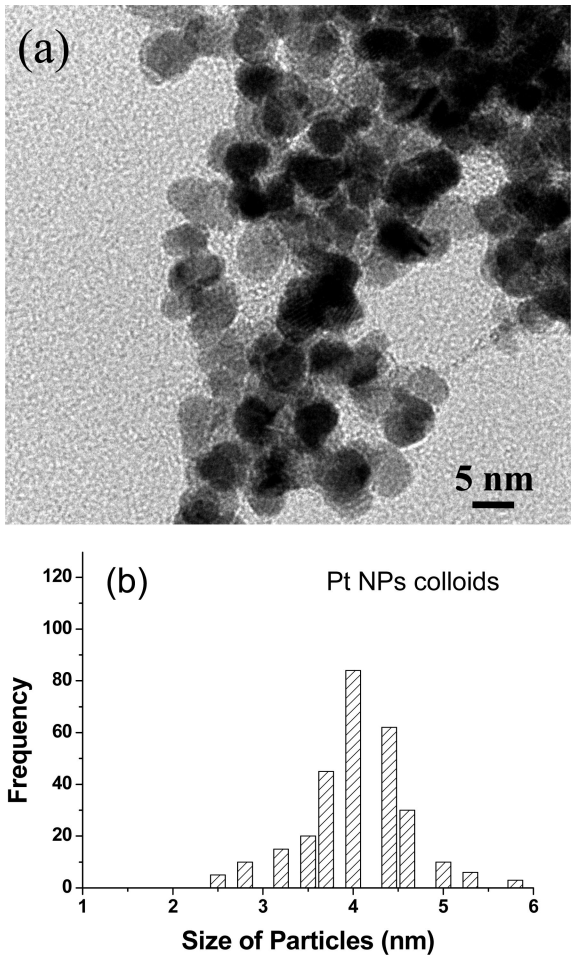

Figure 2. (a) TEM photomicrograph of the Pt NPs from solution and (b) their size distribution in the solution.

ers, or surfactants. The as-synthesized films, with porosities of over 95%, can be handled within reason and can show a high Pt electroactive surface area.

Experimental Section

Chemicals. Hexachloroplatinic acid ($H_2PtCl_6 \cdot 6H_2O$) and formic acid (HCOOH) were used, as received from Sigma-Aldrich. All aqueous solutions were prepared with ultrapure water from a Barnstead Nanopure water system.

Preparation of Pt Porous Film. In a typical synthesis, 0.032 g of $H_2PtCl_6 \cdot 6H_2O$ and 1 mL of HCOOH were added simultaneously to 20 mL of H_2O at room temperature; the amount of HCOOH used is in 400-fold excess, permitting the complete reduction of the H_2PtCl_6 to Pt. The reactions were conducted at 80 °C for ~15 min, the solution turning from golden orange to dark brown in that interval. For self-attachment to the same E-TEK carbon fiber paper (PEMEAS Fuel Cell Technologies, Somerset, NJ) used in their commercial ELAT product, a piece of that paper (~1.5 × 4 cm) was used to raise the Pt layer floating on the upper surface of the solution. Our preliminary studies of film thickness (i.e., the percentage of NPs that form the film) indicate that thickness increases with both temperature and reduction time. We believe that this is at least partly due to the effects of these variables on the size of the CO_2 bubbles produced, and their subsequent loss.

Characterization. The morphology of the porous films was characterized by field emission scanning electron microscopy (FESEM, Hitachi S-4700, operating at 5 kV) and by transmission electron microscopy (TEM, JEOL 2100F, operating at 200 kV). XPS analysis was carried out in a VG ESCALAB II, using a nonmonochromated Al Kα source (1486.6 eV), at a base pressure of 1×10^{-10} Torr. High-resolution spectra were obtained at a perpendicular takeoff angle, using a pass energy of 20 and 0.05 eV steps. The binding energies were calibrated by placing the C(1s) line of adventitious hydrocarbon at 284.6 eV. After Shirley background removal, the component peaks were separated using the XPSPeak Fit program version 4.1.[12]

Electrochemical Measurement. Cyclic voltammetry was performed in pH 1 H_2SO_4 with a standard three-electrode cell at room temperature. The working electrode was prepared by transferring the porous Pt froth film onto ethanol-treated carbon paper (81% porosity), fixed with a 5 wt % Nafion solution (Aldrich) and then dried in air. The Pt loading at the working electrode was measured by neutron activation analysis. A Pt foil was used as the counter-electrode and a saturated calomel electrode was used as the reference electrode. CV measurements were carried out on an EGG 273A potentiostat. Before the measurements were recorded, the electrolyte was purged with N_2 (99.9%) for 30 min, and several tens of CV cycles (sweeping rate: 50 mV/S) were performed to stabilize the electrode surface. The amount of Pt in contact with the electrolyte was measured by integration of the charge related to H adsorption in the cyclic voltammogram, recorded at a sweep rate of 10 mV/s.

Results and Discussion

The synthesis was conducted in aqueous solution, using hexachloroplatinic acid (H_2PtCl_6) as the precursor, and formic acid (HCOOH) as the reducing agent, at 80 °C, using the following chemical reaction:

$$H_2PtCl_6 + 2HCOOH \rightarrow Pt + 6Cl^- + 6H^+ + 2CO_2\uparrow \quad (1)$$

Froth formation is described in Figure 1. As seen there, Pt NPs, produced in solution, float to the upper surface with the escaping bubbles of CO_2, forming a film. A typical TEM image of the as-prepared Pt colloidal NPs, Figure 2, was obtained from drops of the solution, taken from below the film, placed onto a-C film-coated Cu TEM grids and allowed to dry; the figure also contains their size distribution. There is a slight aggregation of the NPs, due to drying in the absence of surfactant. However, the aggregation is dispersed merely on its return to solution, even after several months. Those NPs not brought to the surface by the CO_2 bubbles remain in suspension.

In this light, it should be noted that the use of sodium citrate or mixed formic acid−citrate (9:1) gave no nanoporous films under the same conditions, even after standing for 18 months. This is because citrate is a well-known surface stabilizer for Pt NPs.[13]

(12) http://www.phy.cuhk.edu.hk/~surface/XPSPEAK/
(13) Harriman, A.; Millward, G. R.; Neta, P.; Richoux, M. C.; Thomas, J. M. *J. Phys. Chem.* **1988**, *92*, 1286.

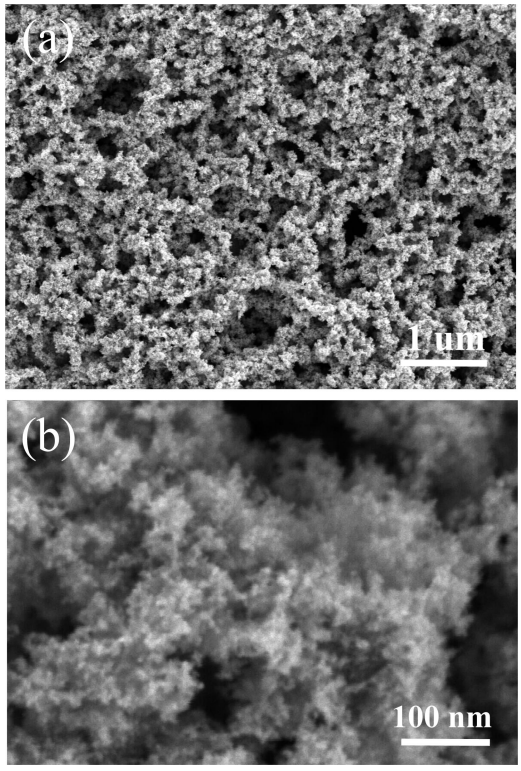

Figure 3. SEM photomicrographs of the porous Pt NP froth at (a) low and (b) high resolutions.

The measured thickness of the froth film at the solution surface increases with reaction time, ultimately attaining a thickness of ~10 μm; under our experimental conditions, it took ~15 min for the complete reduction of the H_2PtCl_6 solution. A typical SEM photomicrograph of the froth is shown in Figure 3, where the pore sizes are seen to range from μm to nm. In addition, our initial results indicate that as the reaction temperature is raised toward 80 °C, the CO_2 bubbles that are formed increase in size, and the measured thickness of the froth film increases.

The film can easily be handled for characterization but its high porosity causes it to have limited mechanical strength and, as a result, it disintegrates under excess compression. The present small size of the froth samples precludes the evaluation of their porosity by macro-sized techniques, so we were forced to estimate it from densities. Such calculations indicate that, in order to float, the Pt thin froth films must have a porosity of at least 95%.

Figure 4 shows TEM photomicrographs of the froth, when removed from the solution surface and placed on a Cu TEM grid. The photomicrographs show the three-dimensional network, with the dimensional distribution of Pt NPs in the network (see Figure 4c), similar to that in Figure 2. Figure 5 contains a TEM photomicrograph of the froth and its selected-area electron diffraction patterns, showing several bright concentric rings, attributed to the (111), (200), (220), and (311) diffractions of the Pt fcc crystal structure.

X-ray photoelectron spectroscopy (XPS) was employed to characterize the surface chemistry of the films. Carbon paper was used as a transfer substrate. An XPS survey scan (not shown) did not detect a Cl(1s) XPS signal, which would have come from residual hexachloroplatinate, indicating that

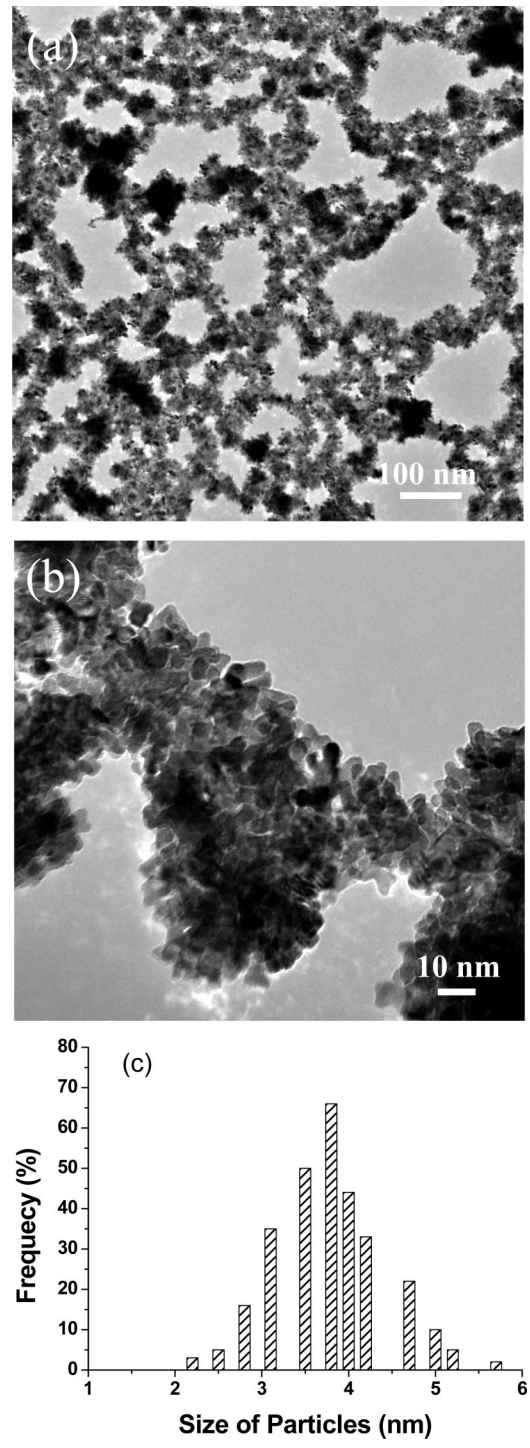

Figure 4. TEM photomicrographs of the porous Pt NP froth at (a) low and (b) high resolutions and (c) the NP size distribution in the froth.

Pt reduction is complete and that no surface stabilizer is electrostatically attached. A high-resolution Pt(4f) XPS doublet is shown in Figure 6, where one notes the absence of a shoulder (due to ions) at the higher binding energy side of each component. This spectrum may be compared with that in our recent publication,[14] where Pt was deposited by evaporation, at 10^{-9} Torr, to form nanoparticles, and ions cannot form; the spectra are identical in terms of peak position, width, and asymmetry, with the asymmetry due to

(14) Yang, D. Q.; Zhang, G. X.; Sacher, E. *J. Phys. Chem. B* **2006**, *110*, 8348.

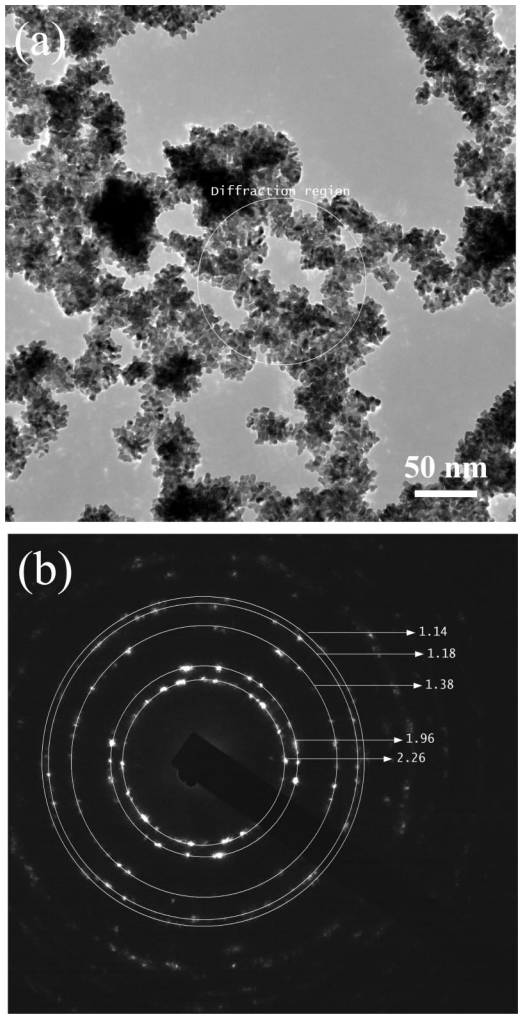

Figure 5. (a) TEM photomicrograph of the porous froth film and (b) its selected area electron diffraction pattern.

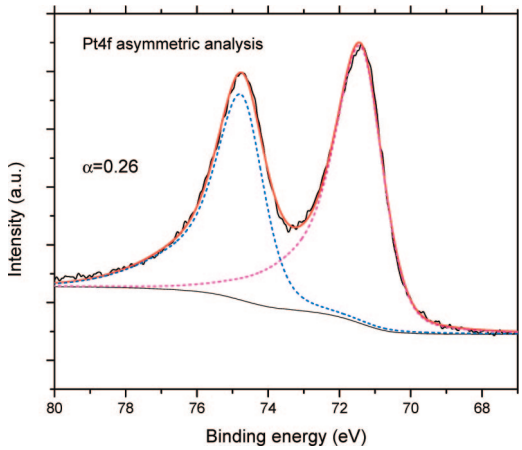

Figure 6. Typical XPS spectrum of the Pt(4f) doublet and its components; α is the peak asymmetry value.

the presence of surface and volume components having different electronic structures, with slightly different binding energies. This is evidence of total reduction, in the present case. The absence of ions means that aggregation and coalescence into the froth occurred through some physical interaction between completely reduced Pt NPs.

The reaction temperature is a key factor in the synthesis of the porous film. We note that, for given concentrations

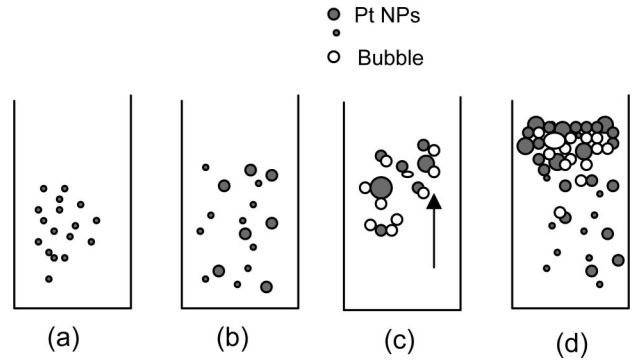

Figure 7. Proposed scheme for porous Pt NP froth formation: (a) Pt NP nucleation and growth, (b) NP formation, (c) the gas bubble entrainment of NPs causes them to rise to the top of the solution, and (d) porous froth formation via NP aggregation and partial coalescence.

of precursor and formic acid, the lower the temperature, the thinner the film; temperatures above 80 °C offered no advantages. It is likely that both kinetic and thermodynamic processes are involved in the reaction. The formation of these films may be separated into three steps, as indicated in Figure 7: (1) the formation of Pt nuclei (Figure 7a), followed by (2) the growth of Pt NPs (Figure 7b), which rise with the CO_2 produced, (3) to form the froth film (Figures 7c,d). Step (3) does not occur in the case of citrate-stabilized Pt NPs[13] because the bubbles do not entrain the NPs.

A mechanism, based on the continuous formation of seeds by rapid autocatalytic growth, has been proposed for the formation of metal NPs, including platinum:[15,16] under our experimental conditions, platinum ions are reduced by formic acid to form platinum NPs, at the early stage of the reduction process. Once the NPs reach a critical size, about 50 atoms,[11] reduction is accelerated through an autocatalytic reduction process.[16,17] The initially nanosized bubbles of CO_2 produced[18] coalesce to form larger bubbles, eventually reaching the buoyancy necessary to rise to the top of the solution, entraining the Pt NPs at the gas−solution interface. The bubble-laden NPs arriving at the surface aggregate to a froth of Pt nanoparticles. That is, the production of CO_2 during the reduction process is a major factor in the formation of the froth.

Froth formation is used, in mining and water purification, for the separation of solid particles from the liquid in which they are dispersed. The particles are entrained at the bubble−liquid interface and rise to the surface to form the froth.[19] When necessary, surfactants are used to aid froth formation.[20]

We note that since large bubbles were not obvious when we used citrate, as described earlier, they may never have reached the buoyancy necessary to rise to the top of the solution. The small bubbles formed either rose, unnoticed, to the surface of the solution or dissolved in it over time, to replace the CO_2 lost from the solution surface. The cleanli-

(15) Liang, H. P.; Zhang, H. M.; Hu, J. S.; Guo, Y. G.; Wangand, L. J.; Bai, C. L. *Angew. Chem., Int. Ed.* **2004**, *43*, 1540.
(16) Greenbaum, E. *J. Phys. Chem.* **1988**, *92*, 4571.
(17) Chen, J. Y.; Herricks, J.; Xia, Y. N. *Angew. Chem., Int. Ed.* **2005**, *44*, 2589.
(18) Cavicchi, R. E.; Avedisian, C. T. *Phys. Rev. Lett.* **2007**, *98*, 124501.
(19) Schwartz, S.; Grano, S. *Colloid Surf. A* **2005**, *256*, 157.
(20) Suzuki, Y.; Maruyama, T. *Water Res.* **2002**, *36*, 2195.

ness of the NP surface and the surface aggregation permit us to offer a possible mechanism for the partial coalescence: as we noted in our previous study of NP coalescence,[21] the liquid-like surface layers of contacting NPs permit interfacial condensation; this releases heat, which permits further melting and coalescence of the NPs. However, a point is ultimately reached where the total size of the coalescing particles is large enough so that the heat released is no longer sufficient to cause further melting; at this point, only partial coalescence will have occurred. For two contacting NPs, this has been found to occur in the 5−10 nm size range,[21] so that any contacting NPs that are larger than this will only partially coalesce. In the present case, any given NP in the froth is surrounded on all sides by other, similar-sized NPs, resulting in a partial coalescence, similar to powder sintering. Those NPs remaining in suspension (Figure 2) evidently have some kind of surface stabilization that prevents them from being entrained at the gas−solution interface and rising. Thus, the bubbles have two functions: (1) to entrain the nanoparticles at the gas−solution interface and (2) to form the froth at the solution−air interface.

The electrochemically active surface area of the froth was measured in H_2SO_4 solution, as described in the Experimental Section. A typical cyclic voltammetry (CV) plot is shown in Figure 8. Features associated with hydrogen adsorption and desorption events, as well as with the reduction of surface oxide, are seen in the plot. Multiple peaks for hydrogen adsorption and desorption are indicative of multiply exposed crystallographic planes.

The electrochemically active surface area (S_{EL}) was quantified by integrating the current associated with these events. The charge value (Q_H), measured under the electroadsorption curve for hydrogen, is 343 mC/cm^2. Neutron activation analysis reveals that the Pt loading in the froth is 0.928 mg/cm^2, giving 369.6 mC/mg Pt. Using the Q_H value and Pt loading, it is possible to calculate the electrochemically active surface area of the froth as

$$S_{EL} = Q_H/(Q_{ref} \times \text{Pt loading}) \quad (2)$$

S_{EL} is obtained in cm^2/mg when the Pt loading is in mg/cm^2; $Q_{ref} = 0.21$ mC/cm^2, corresponding to a surface density of 1.3×10^{15} Pt atoms per cm^2, generally accepted for polycrystalline Pt electrodes.[22] A value of $S_{EL} = 168 \pm 8$ m^2/g is obtained for porous Pt nanostructures. This electrochemically active surface is very large compared with the S_{EL} value of 38 m^2/g Pt measured for a commercial Pt black from Johnson Matthey. As a matter of fact, the S_{EL} value of this Pt froth is equivalent to the best S_{EL} obtained for carbon-supported Pt nanoparticles, for which S_{EL} values up to 180 m^2/g Pt have been reported.[23] These results indicate that a high electrochemically active surface area froth may be obtained without surfactant or stabilizers.

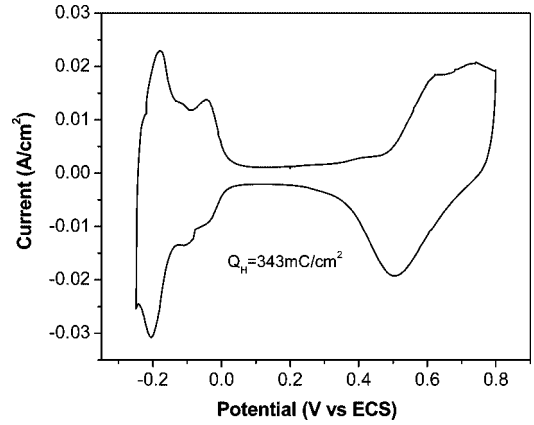

Figure 8. Cyclic voltammetry of a typical porous Pt froth film, deposited onto carbon paper and measured, at a scan rate of 10 mV/s, in deaerated H_2SO_4, at pH 1.

As with any highly porous material, the compressive stress to which it is subjected must be limited.

Conclusions

We have developed an easily implementable procedure to synthesize highly porous Pt thin films, composed of the large-scale assembly of Pt NPs, at relative low temperatures, without the use of surfactants, templates, or stabilizers. The porous thin films exhibit both a high specific surface area and an enhanced electrochemical response that may be useful in various electrochemical applications.

Acknowledgment. The authors thank the Natural Sciences and Engineering Research Council of Canada and GM Canada for funding.

CM800713G

(21) José-Yacamán, M.; Gutierrez-Wing, C.; Miki, M.; Yang, D. Q.; Piyakis, K. N.; Sacher, E. *J. Phys. Chem. B* **2005**, *109*, 9703.

(22) Woods, R. *J. Electrochem. Soc.* **1976**, *9*, 1.

(23) Stonehart, P. *Ber. Bunsen-Ges Phys. Chem.* **1990**, *94*, 913.